PROGRAMME OF THE EUROPEAN UNION

copernicus Europe's eyes on Earth

EUMETSAT

co-funded with esa

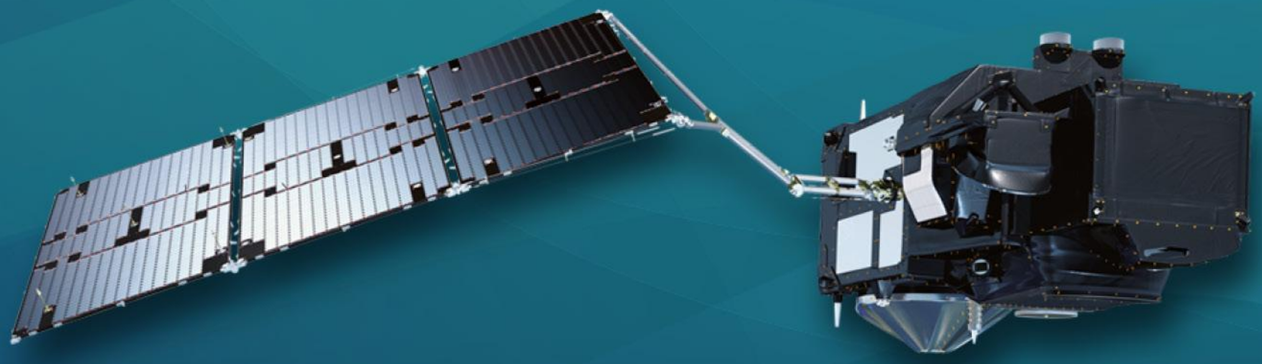

9th Sentinel-3 Validation Team meeting 2026

30 March–01 April 2026 | ESA–ESRIN | Frascati (Rome), Italy

This work was carried out as part of the project ESA S3VT PP0097749 (T-based and R-based validation of the Sentinel-3 SLSTR LST product and an alternative emissivity-dependent split-window algorithm).

EVALUATION OF THE CALIBRATION OF THE SLSTR TIR BANDS AND LST PRODUCTS

R. Niclòs[1], J. Puchades[1], Ll. Pérez-Planells[2], C. Coll[1], S. Arribas[1], F.M. Göttsche[3] & J.A.Valiente[2]

1- Thermal Remote Sensing Group, Department of Earth Physics and Thermodynamic, University of Valencia, Spain
2- Mediterranean Center for Environmental Studies (CEAM), Spain
3- IMK-ASF, Karlsruhe Institute of Technology (KIT), Germany

Outline

1. Objective
2. Ground measurements
3. Calibration of thermal bands
4. Operational SLSTR LST and alternative E-SW algorithm
5. T-based and R-based methods
6. Sites
7. Results: calibration, T-based and R-based validation
8. Conclusions

1. Objective

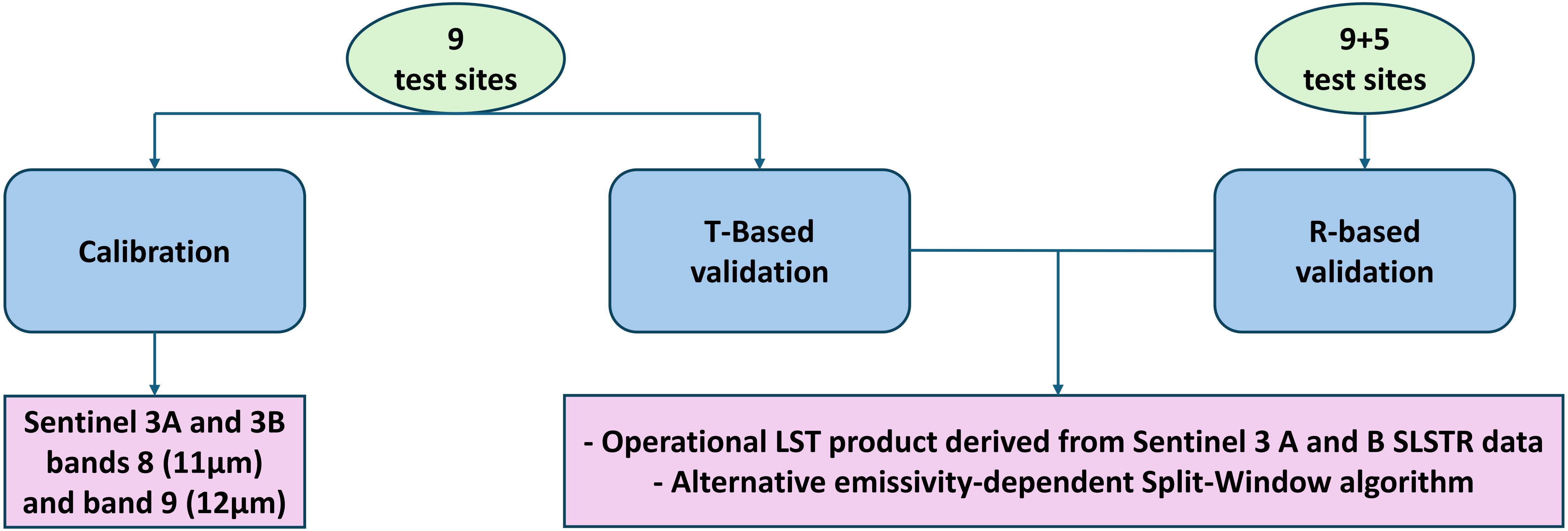

The Global Climate Observing System (GCOS) recommends an uncertainty threshold for satellite-retrieved LST of:

- ±1 K for accuracy (i.e. systematic uncertainty)
- ±1 K for precision (i.e. random uncertainty)

2. Ground LST measurement

Ground LST (T_g) was derived from:

$$L_i^{sen} = \varepsilon_i B_i(T_g) + (1 - \varepsilon_i) L_i^{\downarrow}(\theta)$$

where

- L_i^{sen} is the ground-leaving radiance measured in homogeneous sites using Apogee SI-121 or Heitronics KT15.85 IIP radiometers.
- $L_i^{\downarrow}(\theta)$ is the downwelling sky radiance measured at the sites (considering an effective angle around 53º for Lambertian surfaces or the complementary angle for specular surfaces).
- ε_i is the surface emissivity measured using multiband radiometers and applying TES (Gillespie et al., 1998) or Box methods (Rubio et al., 2003).

Gillespie, A.; Rokugawa, S.; Matsunaga, T.; Cothern, J.S.; Hook, S.; Kahle, A.B.. A temperatura and emissivity separation algorithm for advanced spaceborne termal emisión and reflection radiometer (ASTER) images, IEEETrans. Geosci. RemoteSens. 1998,vol.36,pp.1113–1126
Rubio, E.; Caselles, V.; C.Coll; Valor, E.; Sospedra, F.. Thermal-infrared emissivites of natural surfaces: Improvements on the experimental set-up and new measurements, Int.J.RemoteSens., 2003, vol.24, pp.5379–5390.

3. Calibration of thermal bands

PROGRAMME OF THE EUROPEAN UNION | copernicus | EUMETSAT | co-funded with esa

Comparison of satellite BTs with simulated BTs from ground measured LSTs (T_g), emissivity data and atmospheric profiles.

Simulated at sensor radiance for bands i=8 and 9 (L_i^{sen}) according to:

$$L_i^{sen} = \left[\varepsilon_i B_i\left(T_g\right) + (1 - \varepsilon_i)L_i^{\downarrow}\right]\tau_i(\theta) + L_i^{\uparrow}$$

where:

ε_i is the emissivity

$L_i^{\downarrow}$ is the sky radiance

τ_i is the atmospheric transmittance

$L_i^{\uparrow}$ is the upwelling atmospheric radiance

θ is the satellite zenith angle

Atmospheric transmittances and radiances were simulated from NCEP atmospheric profiles with MODTRAN 5.2

4. Operational SLSTR LST algorithm

Algorithm for the operational SLSTR LST L2 product described in the SLSTR LST ATBD:

$$T = a_{f,i,wvc} + b_{f,i}(T_8 - T_9)^{\sec(\theta/m)} + (b_{f,i} + c_{f,i})T_9$$

where:

- T is the LST
- T_8 and T_9 are the brightness temperatures at 10.8 µm and 12.0 µm (bands S8 and S9)
- θ is the satellite zenith angle
- m is a parameter related to θ
- $a_{f,i,wvc}$, $b_{f,i}$ and $c_{f,i}$ are algorithm coefficients which depend on:
  - Surface biome (*i*)
  - Vegetation Cover Fraction (*f*)
  - Water vapor content (*WVC*)
  - Day/night time (only water)

Sentinel-3 Optical Products and Algorithm Definition: SLSTR Land Surface Temperarure Algorithm Theoretical Basis Document (ATBD), 2012. [Online]. Available on: https://sentinel.esa.int/documents/247904/349589/SLSTR_Level-2_LST_ATBD.pdf.

4. Alternative E-SW algorithm

PROGRAMME OF THE EUROPEAN UNION | copernicus | EUMETSAT | co-funded with esa

Alternative emissivity dependent Split-Window algorithm:
- First proposed by Niclòs et al. (2011)
- Adapted to Sentinel-3 SLSTR data in Pérez-Planells et al. (2021):

$$T = T_8 + a_0 + a_1(\sec(\theta) - 1) + \big(a_2 + a_3(\sec(\theta) - 1)\big)(T_8 - T_9)$$
$$+\big(a_4 + a_5(\sec(\theta) - 1)\big)(T_8 - T_9)^2 + \alpha(1 - \varepsilon) - \beta\Delta\varepsilon$$

where:
- T is LST
- T_8 and T_9 are the brightness temperatures at 10.8 µm and 12.0 µm
- $\varepsilon = 0.5(\varepsilon_8 + \varepsilon_9)$ and $\Delta\varepsilon = \varepsilon_8 - \varepsilon_9$
- a_i are the E-SW coefficients
- θ is the satellite zenith angle
- $\alpha = (a_6 + a_7 W + a_8 W^2)$ and $\beta = (a_9 + a_{10} W)$
- $W = WVC/\cos(\theta)$

SWA Coefficients	
a_0 (K)	0.052 ± 0.013
a_1 (K)	0.15 ± 0.02
a_2	0.95 ± 0.02
a_3	-0.30 ± 0.03
a_4 (K^1)	0.305 ± 0.004
a_5 (K^{-1})	0.202 ± 0.007
a_6 (K)	52.51 ± 0.18
a_7 (K cm^{-1})	-0.11 ± 0.12
a_8 (K cm^{-2})	-1.004 ± 0.018
a_9 (K)	75.7 ± 0.2
a_{10} (K cm^{-1})	-11.21 ± 0.06

Niclòs, R.; Galve, J.M.; Valiente, J.A.; Estrela, M.J.; Coll, C. Accuracy assessment of land Surface temperatura retrievals from MSG2-SEVIRI data. Remote Sens. Environ.2011,115,2126–2140.
Pérez-Planells, L.; Niclòs, R.; Puchades, J.; Coll, C.; Göttsche, F.-M.; Valiente, J.A.; Valor, E.; Galve, J.M. Validation of Sentinel-3 SLSTRL and Surface Temperature Retrieved by the Operational Product and Comparison with Explicitly Emissivity-Dependent Algorithms. RemoteSens.2021,13,2228.

5. T-based and R-based method

- The **Temperature-based** method implies the comparison of satellite LSTs with ground measured LSTs.

-The **Radiance-based** method (Wan and Li, 2008) is applied when no ground measurements of LSTs are available:

1.Using at sensor radiances in bands 10.8 μm and 12 μm, atmospheric parameters (derived from interpolated NCEP profiles with the MODTRAN code) and emissivity data, the LST is obtained for both bands, T_{g8} and T_{g9}, through:

$$B_i(T_{gi}) = \frac{L_i^{sen} - L_i^{\uparrow}}{\tau_i \varepsilon_i} - \frac{(1-\varepsilon_i)L_i^{\downarrow}}{\varepsilon_i}$$

2. The differences $\delta = T_{g8} - T_{g9}$ are calculated and only cases for which δ is within a small interval around zero (±0.7 K) are selected as valid cases.

3. For the valid cases, the temperatures calculated for the 10.8 μm band, T_{g8}, are considered as the reference LSTs for comparison with the satellite LSTs.

Wan, Z., Li, Z.L., 2008. Radiance-based validation of the V5 MODIS land-surface temperature product. Int J Remote Sens 29, 5373–5395.

6. Sites for T-based validation

Rice field

~100-km^2 rice field area located near Valencia city, Spain
1) Bare soil: from February to May
2) Water (flood): December, January and June
3) Full vegetation: July to mid-September

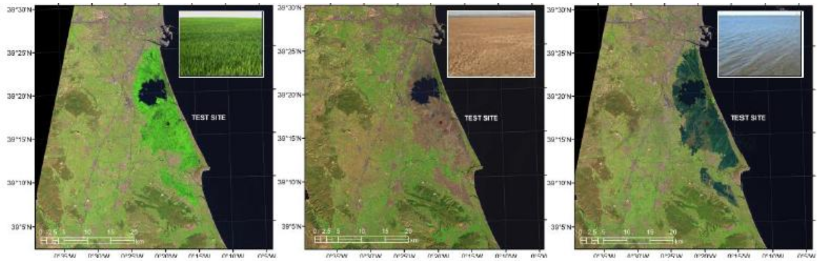

Land cover: post-flooding or irrigated cropland (biome 1)

Gobabeb

Located in Gobabeb, Namibia.
Arid desert site, which is highly stable in space and time.

Land cover: bare area, unknown (biome: 20)

Shrubland

~200 km^2, high-plain area (site elevation of 800 m above sea level) of dense shrubland. Seasonally invariant.

Land cover: closed to open (>15%) shrubland (<5m) (biome: 13)

Lake Constance

Lake water surface temperature measurements with ship borne infrared radiometers (Heitronics KT15.85IIP).

Land cover: Water bodies (biome: 26)

6. Sites for T-based validation

Five stations set up in previously unrepresented forest biomes from the **Copernicus Space Component LAW network**:

- **KIT Forest** (**Biome: 6**), in Karlsruhe, Germany. Closed broadleaved deciduous forest biome according to the SLSTR product.
- **Hyytiälä (HYY)** (**Biome: 10**), in the Juupajoki forest, Finland, classified as mixed forest.
- **Puéchabon (PUE)** (**Biome: 15**), in a forest area in South France classified as sparse vegetation
- **Svartberget (SVA)** (**Biome: 9**), in an experimental forest in Sweden classified as open needle leaved forest.
- **Robson Creek (ROB)** (**Biome: 5**), in a rainforest area in Australia classified as broadleaved evergreen forest.

KIT Forest

Svartberget

Robson Creek

6. Sites for R-based validation

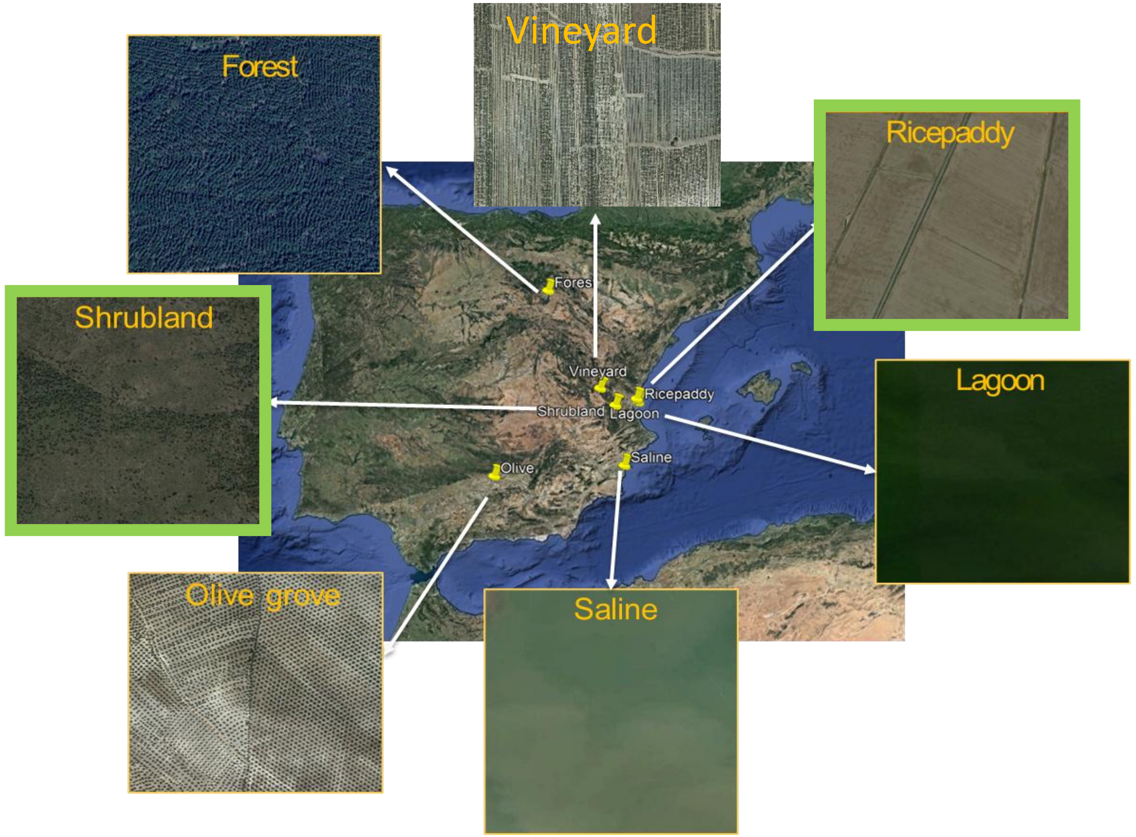

Two years of data (2021-2022)

Emissivity for SLSTR band i:

$$\varepsilon_i = \varepsilon_{vi} f + \varepsilon_{si}(1-f) + 4(-0.435\varepsilon_{si} + 0.4343)(1-f)f$$

(Valor and Caselles, 1996) (Pérez-Planells et al., 2022)

Site	Biome	Vegetation emissivity (ε_{vi})		Soil emissivity (ε_{si})	
		Band 8	Band 9	Band 8	Band 9
Lagoon & saline*	26	N/A	N/A	N/A	N/A
Ricepaddy	1	0.985	0.980	0.970 (0.972)*	0.972 (0.977)*
Shrubland	13	0.985	0.986	0.972	0.977
Forest	8	0.977	0.977	0.972	0.977
Vineyard	2	0.972	0.973	0.967	0.959
Olive grove	15	0.976	0.976	0.967	0.959

*Values in parentheses for wet bare soil

Biomes:
1 =post-flooding or irrigated cropland
2 = rainfed croplands
8 = closed (>40%) needleleaved evergreen forest (>5m)
13 = closed to open (>15%) shrubland (<5m)
15 = Sparse vegetation (>15%) (Woody vegetation, shrubs, grassland)
26 = water bodies

Valor, E. and Caselles, V., (1996). Mapping land Surface emissivity from NDVI: Application to European, African and South American areas. Remote Sensing of Environment, vol.57, no.3, pp.167–184.
Pérez-Planells, L.; Niclòs, R.; Valor, E.; Göttsche, F.-M., (2022). Retrieval of land Surface emissivities over partially vegetated surfaces from satellite data using radiative transfer models. IEEE Transactions on Geoscience and Remote Sensing, Vol.60, 500382
***Niclòs, R.; Caselles, V.; Valor, E.; Coll, C. and Sánchez, J.M. (2009). A simple equation for determining sea Surface emissivity in the 3–15µm. International Journal of RemoteSensing, 30(6),1603–1619.**

7. Results: calibration

Statistical results for the differences between satellite and simulated BT.

		Sentinel-3A			Sentinel-3B		
Site	**Bands**	**Median (K)**	**R-RMSD (K)**	**Match-up number**	**Median (K)**	**R-RMSD (K)**	**Match-up number**
Shrubland	**Band 8**	0.3	1.4	86	0.6	1.5	85
	Band 9	0.3	1.4		0.5	1.4	
Rice paddy	**Band 8**	0.3	0.7	136	0.3	0.7	124
	Band 9	0.2	0.7		0.3	0.7	
KIT	**Band 8**	-0.3	0.6	130	-0.3	0.5	158
	Band 9	-0.1	0.5		-0.0	0.5	
Gobabeb	**Band 8**	-0.3	0.4	87	-0.3	0.4	136
	Band 9	0.0	0.3		-0.2	0.3	
Lake_Constance	**Band 8**	-0.4	0.6	54	-0.4	0.6	60
	Band 9	-0.4	0.6		-0.3	0.4	
HYY	**Band 8**	-0.9	1.2	112	-1.0	1.3	113
	Band 9	-0.7	1.0		-0.7	1.0	
PUE	**Band 8**	-0.2	0.7	152	-0.2	0.7	166
	Band 9	0.0	0.7		0.1	0.7	
ROB	**Band 8**	-0.2	0.7	49	-0.2	0.8	65
	Band 9	-0.2	0.5		-0.2	0.8	
SVA	**Band 8**	-0.6	1.0	118	-0.7	1.1	116
	Band 9	-0.5	0.9		-0.5	1.0	
Total	**Band 8**	-0.3	**0.8**	**924**	-0.3	**0.8**	**1023**
	Band 9	-0.2	**0.7**		-0.1	**0.7**	

Satellite BTs against simulated BTs. Data is grouped by biome.

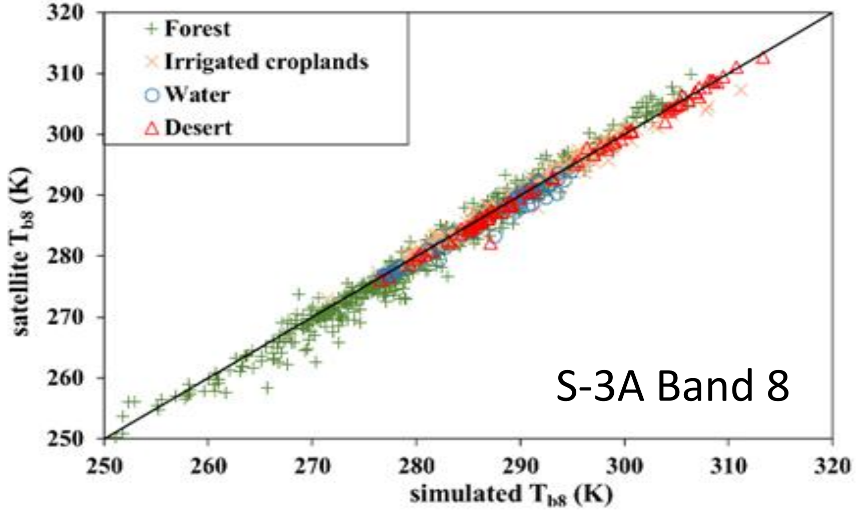

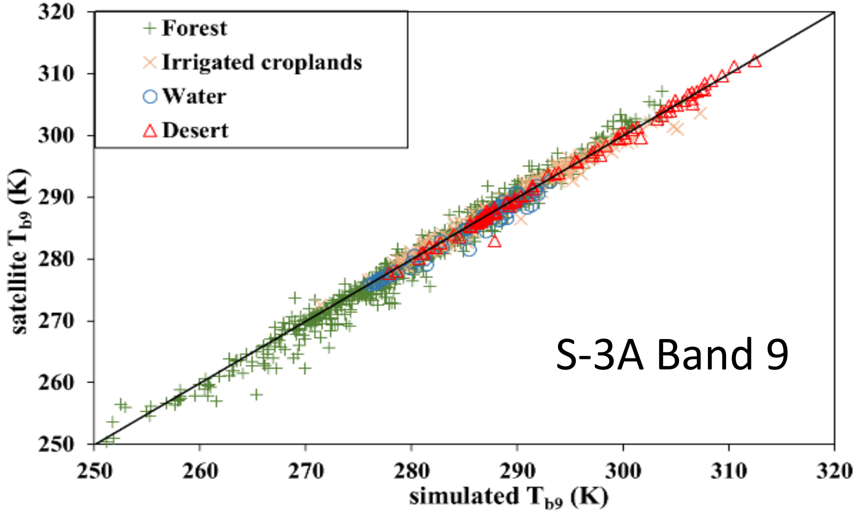

7. Results: T-based validation

Statistical results for the differences between satellite and ground measured LSTs

Biome	Results (K)	SLSTR product		E-SW	
		S-3A	S-3B	S-3A	S-3B
Lake (Day)	Median	0.3	0.2	-0.5	-0.7
	R-RMSD	0.7	0.9	0.7	0.9
Desert (All)	Median	-2.1	-2.2	-1.0	-0.6
	R-RMSD	2.2	2.3	1.6	1.3
Irrigated cropland (All)	Median	1.6	2.0	0.1	0.2
	R-RMSD	1.8	2.2	0.9	0.8
Forest (All)	Median	0.0	0.1	-0.6	-0.6
	R-RMSD	1.3	1.3	1.3	1.3

Dependence of LST biases on WVC and ground LST for desert and irrigated croplands for S-3A

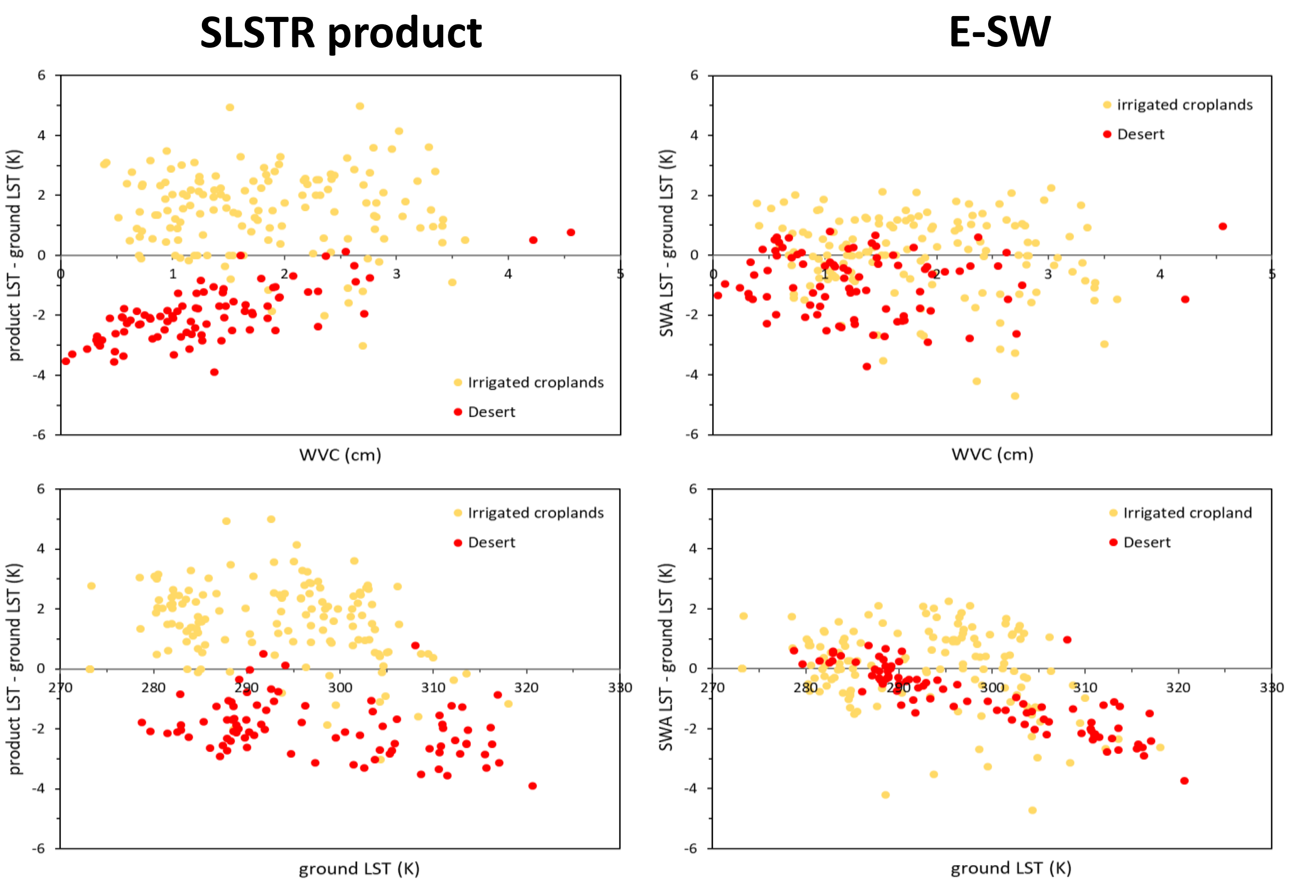

7. Results: R-based validation

Statistical results for the differences between satellite and reference data (R-based)

Biome	Results (K)	SLSTR product		E-SW	
		S-3A	S-3B	S-3A	S-3B
Lake	Median	0.7	0.6	-0.1	-0.1
	R-RMSD	0.9	0.9	0.4	0.4
Desert	Median	-1.7	-1.7	-0.1	0.0
	R-RMSD	1.8	1.8	1.2	1.3
Irrigated cropland	Median	1.6	1.5	-0.1	-0.1
	R-RMSD	1.7	1.7	0.3	0.3
Forest	Median	0.4	0.5	-0.2	-0.2
	R-RMSD	0.7	0.8	0.3	0.3
Sparse vegetation	Median	0.3	0.6	-0.1	-0.1
	R-RMSD	0.6	0.9	0.9	0.6
Rainfed cropland	Median	1.0	0.9	-0.1	0.0
	R-RMSD	1.1	1.2	0.4	0.5

Dependence of LST biases on WVC and R-based LST for desert, irrigated croplands and rainfed croplands for S-3A

SLSTR product **E-SW**

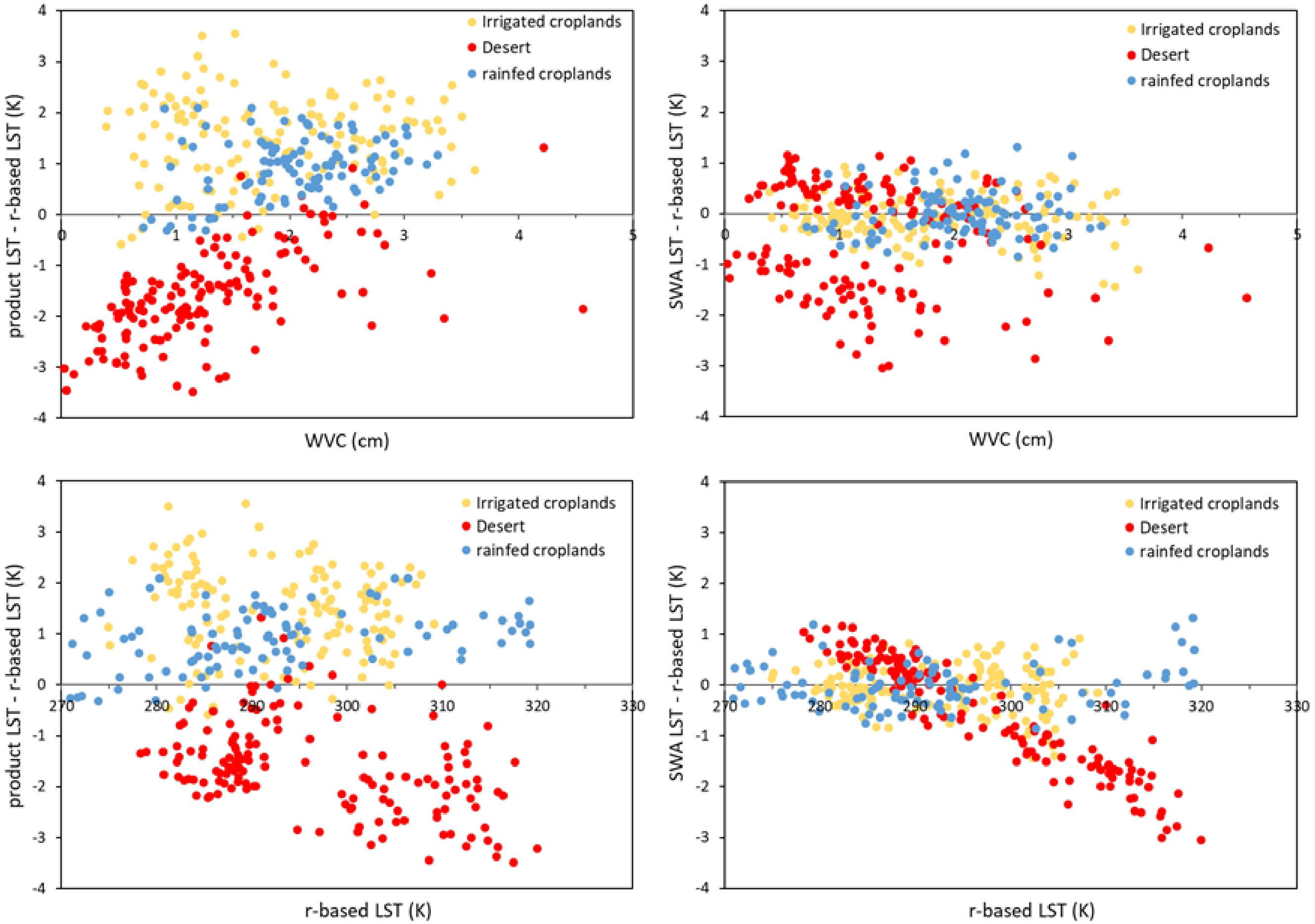

8. Conclusions

- R-RMSD **between simulated and satellite brightness temperatures** for both SLSTR sensors (3A and 3B) were **0.8 K and 0.7 K for band 8 and 9**, respectively, which were within the uncertainty limits of the simulated brightness temperatures.
- The **validation** of the operational SLSTR product and the E-SW LST **yielded consistent results** for Sentinel-3A and 3B.
- For the **T-based method**, the **operational SLSTR LST product showed overall R-RMSD of 1.6 K**, with mean biases exceeding the recommended ±1.0 K threshold for desert (-2 K) and irrigated croplands (1.5 K).
- For the **E-SW, R-RMSDs were 1.3 K**, the desert site (daytime) being the only case with excessive bias (-1.5 K).
- The **R-based method** results confirmed the large biases in the above mentioned cases, showing overall **R-RMSDs of 1.0 K for the operational SLSTR LST product and of 0.5 K for the E-SW**, which were lower than for the T-based validation.

Puchades, J., Niclòs, R., Pérez-Planells, Ll., Coll, C., Göttsche, F.M., Valiente, J.A. & Valor, E. (2025). Ground Calibration of Sentinel-3 SLSTR Thermal Infrared Bands and Validation of LST Algorithms. GIScience & Remote Sensing (under review).

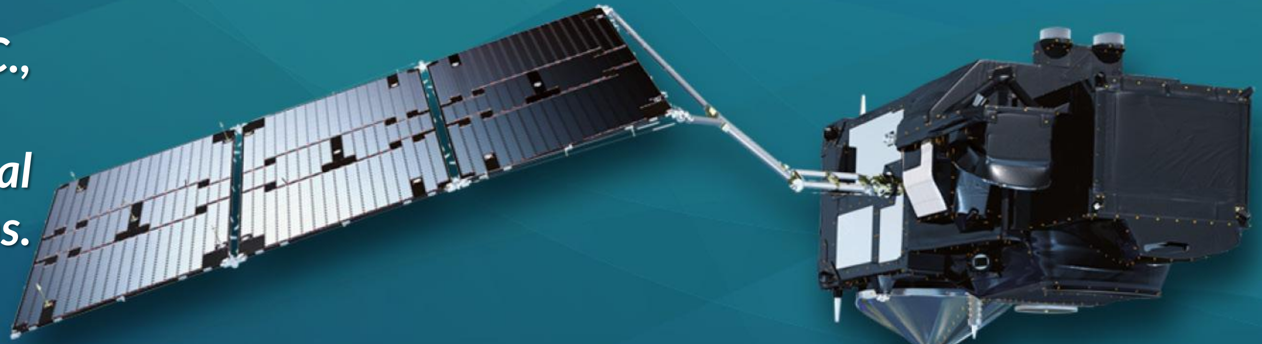

9th Sentinel-3 Validation Team meeting 2026

30 March–01 April 2026 | ESA–ESRIN | Frascati (Rome), Italy

Thank you!
Questions are welcome.

Evaluation of the calibration of the SLSTR TIR bands and LST products

R. Niclòs[1]*, J. Puchades[1], Ll. Pérez-Planells[2], C. Coll[1], <u>S. Arribas[1]</u>, F.M. Göttsche[3] & J.A.Valiente[2]

1- Thermal Remote Sensing Group, Department of Earth Physics and Thermodynamic, University of Valencia, Spain; * **raquel.niclos@uv.es**
2- Mediterranean Center for Environmental Studies (CEAM), Spain
3- IMK-ASF, Karlsruhe Institute of Technology (KIT), Germany

Acknowledgments:

This work was carried out as part of the project ESA S3VT PP0097749 (T-based and R-based validation of the Sentinel-3 SLSTR LST product and an alternative emissivity-dependent split-window algorithm). Sara Arribas' participation is supported by the Generalitat Valenciana (CIACIF/2023/525), co-funded by the European Social Fund Plus (ESF+).